

UDK 620.193:691.328

FRACTURE TOUGHNESS OF THE HIGH-STRENGTH STEELS WITHIN THE DUCTILE TO CLEAVAGE TRANSITION TEMPERATURE RANGE – MASTER CURVES

A. NEIMITZ, I. R. DZIOBA

Kielce University of Technology, Poland

Fracture toughness of high-strength ferritic steels within the ductile to cleavage transition temperature range was analyzed. Two steels S960QC and Hardox-400 were tested. The experimental results were compared with those received by the standard Master Curve (MC) equation. It turns out that the MC equation can be adopted to predict the fracture toughness of the high-strength steels after some modifications. The shape of the formula can be preserved, but some coefficients should be changed. The relation between the fracture toughness and the element thickness which is included in the MC formula does not exist in the case of the high-strength steels. One formula for the MC for the tested steels cannot be proposed, in contrast to the steels with a yield stress below 825 MPa.

Keywords: *fracture toughness, Master Curve, high-strength steels, thickness effect, ductile to brittle transition.*

The classical Master Curve (MC) establishes the relationship between the fracture toughness and temperature within the cleavage to ductile transition temperature range for ferritic steels with a yield stress in the range 275...825 MPa. The method of determining the transition temperature, T_0 , and the technique of finding these curves was presented in a series of works [1–6], in the ASTM E 1921-05 standard [7] and in the FITNET procedure [8]. The classical MC in extended by Wallin and Nevasmaa [9] and Bannister [10] form can be written as follows:

$$K_{\text{mat}} = K_{\text{min}} + \left\{ 11 + 77 \exp(0.019[T - T_0 + \Delta T_K]) \right\} \left(\frac{B_1}{B_2} \right)^{0.25} \left[\ln \left(\frac{1}{1 - P_f} \right) \right]^{0.25}, \quad (1)$$

where $\Delta T_K = 13(0.5 - P_f)$; P_f is the probability of fracture; B_1 and B_2 are the thicknesses of the specimens or structural elements and usually B_2 is considered as the reference thickness which is assumed to be equal to 25 mm; $K_{\text{min}} = 20 \text{ MPa}\cdot\text{m}^{1/2}$ and T is the test temperature. At the reference temperature, T_0 , the critical stress intensity factor is assumed to be $K_{\text{mat}} = 100 \text{ MPa}\cdot\text{m}^{1/2}$. If $P_f = 0.5$ and $B_1 = B_2 = 25 \text{ mm}$ the MC can be written in a simpler form:

$$K_{\text{mat}} = K_{25(B)} = 30 + 70 \exp[0.019(T - T_0)]. \quad (2)$$

The fracture toughness data obtained for the original specimen thicknesses should be converted to 25 mm thickness according to equation [7, 8]:

$$K_{\text{mat}} = K_{\text{min}} + (K_B - K_{\text{min}})(B/25)^{0.25}. \quad (3)$$

During recent years new ferritic steels have been designed and produced which are characterized by their high yield stress values, greater than 825 MPa (e.g. S960QC, Hardox-400 [11, 12]). To achieve such a high strength these steels are subjected to thermo-

mechanical treatment. The first tests made on the S960QC showed that the MC obtained according to the ASTM E 1921-05 procedure did not fit the experimental results properly [13]. There are several reasons for this behavior. One of these is due to the rolling and heat treatment technologies which are aimed at producing a yield stress $\sigma_y \geq 960$ MPa for each plate thickness. This results in small differences in the microstructure for different plate thicknesses. These differences lead to the fracture toughness changing in such a way that the influence of the plate thickness on the fracture toughness cannot be uniquely established [13, 14].

The microstructure of the high-strength ferritic steels is tempered bainite-martensite. The microstructure of the ferritic steels with yield strength less than 825 MPa is ferrite-pearlite-bainite or ferrite-bainite. The strength and fracture toughness of the bainite-martensite steels are considerably higher than the ferrite-pearlite-bainite or ferrite-bainite steels [15, 16]. This is one reason that the fracture toughness at the ductile to brittle transition temperature is also higher [13, 14]. In the case of the S960QC steel, the cleavage fracture is observed at -50°C and at this temperature $K_{Jc} \approx 165\div 170 \text{ MPa}\cdot\text{m}^{1/2}$. As a result of the research program the following modified formula for the MC for this steel was proposed [13, 14]:

$$K_{Jc} = (A + B) + \{C^* \exp[D(T - T_{\text{trans}})]\} \cdot \left[\ln \left(\frac{1}{1 - P_f} \right) \right]^{0.25} \quad (4)$$

where $T_{\text{trans}} = -50^\circ\text{C}$; $A = 20$; $B = 15$; $C^* = 145$; $D = 0.016$.

This paper presents the results of experiments on the determination of the MC for high-strength Hardox-400 steel. The aim was to confirm or to reject the conclusions following from the tests carried out on the S960QC steel.

Materials and tensile properties. The specimens for fracture toughness tests were cut out from 30 mm thick plates made of Hardox-400 steel. The plates were produced using a controlled thermo-mechanical treatment. As a result of this treatment the hardness distributions through the thickness as well as the tensile properties are not uniform (Fig. 1). In the middle part of the plate the hardness level is $\sim 350 \text{ HV}_{10}$ and near the surface it is $\sim 400 \text{ HV}_{10}$. The microstructure of the Hardox-400 steel is tempered base metal (BM). The grain sizes are within the range $5 \dots 20 \mu\text{m}$ (Fig. 2). Numerous precipitates of sizes $50 \dots 300 \text{ nm}$ and separate large inclusions ($1.0 \dots 1.5 \mu\text{m}$) are observed.

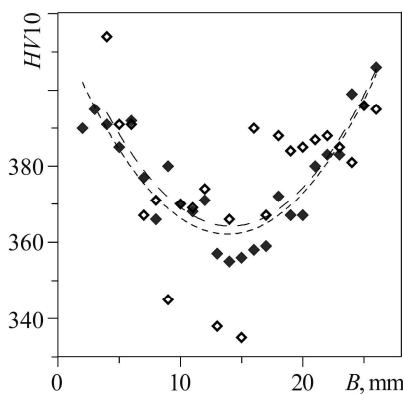


Fig. 1.

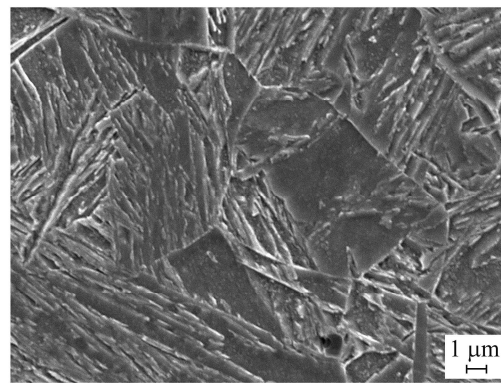


Fig. 2.

Fig. 1. Hardness distribution through the thickness in the plates of Hardox-400 steel.

Fig. 2. Microstructure of Hardox-400 steel; $\times 5000$.

The tensile tests were performed on a cylindrical standard specimen with a diameter equal to 5 mm and length of 25 mm (Fig. 3). The yield and ultimate stresses decrease linearly with the test temperature for Hardox-400 steel (Fig. 4). The regression lines for tensile test data as a function of temperature were determined and later during fracture toughness results analysis.

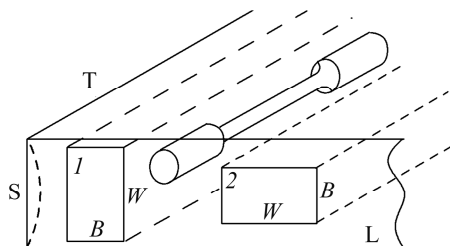


Fig. 3.

Fig. 3. Scheme of cutting tensile and SEN(B) specimens for T-S direction (1) and T-L direction (2).

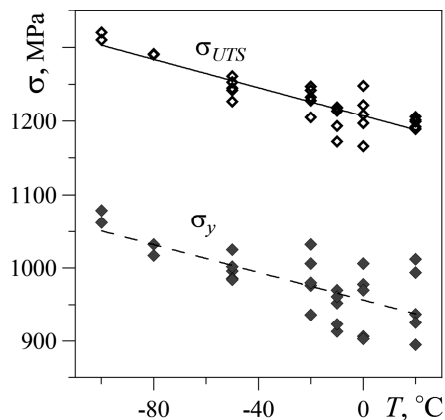


Fig. 4.

Fig. 4. Yield stress σ_y and ultimate stress σ_{UTS} vs. temperature data for the Hardox-400 steel: $\sigma_y = -0.96T + 955.46$ and $\sigma_{UTS} = -0.96T + 1207.14$.

Fracture toughness tests. The Hardox-400 steel was available in plates of 30 mm thickness (Fig. 3). The single etch notched (SEN(B)) specimens with transversal-short-transversal (T-S) orientation were machined in such a way that the crack fronts were always located in the middle of the plate. Thus, microstructure and tensile properties were always the same for the specimens of different thicknesses. The thicknesses of the specimens of T-S orientation were $B = 4; 8; 12; 16; 20; 24$ mm and $a/W = 0.5$. The tests on the specimens of transversal-longitudinal (T-L) orientation were performed on the specimens with a thickness of 6; 8 and 12 mm and $a/W = 0.5$. They were carried out to compare the results with those obtained for similar specimens of the S960QC steel [13, 14]. In the case of the S960QC steel the specimens for fracture toughness tests, SEN(B), were machined in the T-L direction only, because the maximum plate thickness was 8 mm and selection of the T-S orientation, to avoid the non-uniform hardness distribution, was not possible.

Fracture toughness was measured within the temperature range $[-100; 20^\circ\text{C}]$ using the J -integral definition and the standard recommendations [17, 18].

The fatigue pre-cracking of the specimens made of the steels tested in the research program was performed according to the ASTM Standard E1820 09, point 7.4. The ductile to cleavage transition (reference) temperature is not denoted by T_0 as in the Standard E1921 but by T_Q . It is so because the requirements concerning the specimen thickness were not satisfied; namely $B \neq W$ or $2B \neq W$ and $B \neq 25$ mm. However, in Eq. 1 the thickness correction according to FITNET [8] was introduced and the plane strain requirement was always satisfied.

The reference temperature T_Q was computed when the fracture toughness reached $100 \text{ MPa}\cdot\text{m}^{1/2}$. However, this fracture toughness was always reached at very low temperatures, when the fracture process was totally cleavage. Thus, the transition temperature in Eq. (4), T_{trans} , was assessed differently but not arbitrarily. After each test the fracture surface was examined by a scanning microscope. When the cleavage was

preceded by ductile fracture, covering the area of about 50...80 μm in length, the fracture toughness and the temperature were considered as reference values. All fracture toughness results presented in this paper are converted to the stress intensity factor units using the well-known formula: $K_{Jc} = \sqrt{E \cdot J_{Ic} / (1 - \nu^2)}$, where J_{Ic} is a critical value of J -integral, E is Young's modulus, ν is Poisson's ratio.

The fracture toughness vs. temperature dependences for the specimens with T-L orientation for the specimen thicknesses $B = 6; 8$ and 12 mm are shown in Fig. 5a. These results converted to the 25 mm reference specimen thickness (Eq. (3)) are presented in Fig. 5b. The solid lines were obtained using the classical MC (Eq. (1)) with the failure probability $P_f = 0.5$. The dashed lines represent the exponential regression function for experimental data according to the thickness.

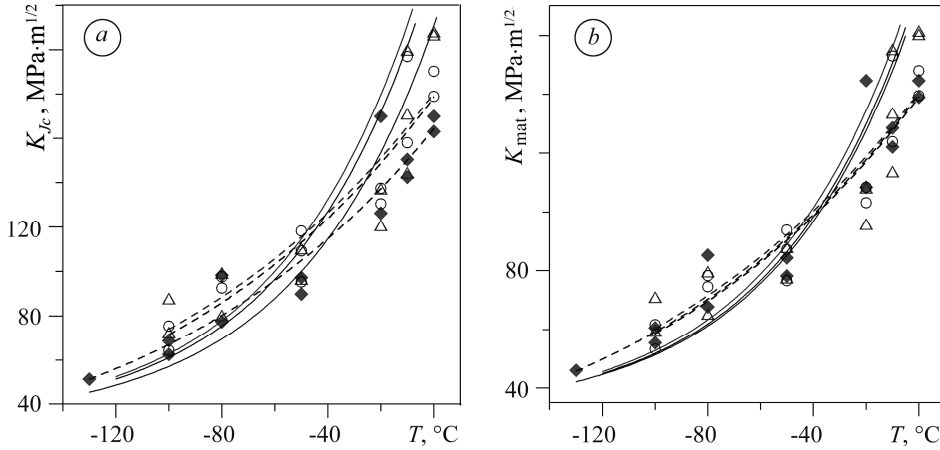


Fig. 5. K_{Jc} vs. temperature, results presented for the original specimen thicknesses (a) (\blacklozenge – $B = 12$ mm, \triangle – $B = 8$ mm, \circ – $B = 6$ mm) and K_{mat} vs. temperature, results after conversion to 25 mm thickness (b).

These results confirm the observations obtained for the S960QC steel [13, 14]. The classical MC runs higher than the experimental points for the temperature in the range $T > -30^\circ\text{C}$. It was also shown that for the specimens with T-L orientation there is no clear dependence between the fracture toughness and the specimen thickness. It was observed earlier [13, 14] and it is confirmed now that the microstructure and tensile properties variation through the specimen thickness dominates the expected fracture toughness – thickness relationship.

To eliminate the supposed microstructure influence on the fracture toughness – thickness relationship, the fracture specimens with T-S orientation were used in the tests. Results were obtained for the specimens with thickness varying from 4 to 24 mm. First results on this subject were presented in paper [19]. It turns out that when the specimens with T-S orientation are used, the fracture toughness – specimen thickness, $K_{Jc} - f(B)$, dependence is observed; however, it does not follow Eq. (1) exactly (Fig. 6). All results and the exponential regression lines for each thickness are shown in Fig. 6a.

The dependence of the fracture toughness on the thickness can be clearly seen in Fig. 6b. The most pronounced dependence between the fracture toughness and the specimen thickness can be observed at $T_{test} = 0^\circ\text{C}$. It becomes weaker for lower temperatures (Fig. 6b). The data points in Fig. 6b were approximated by regression power functions. The data points in Fig. 6b can be also approximated by Eq. (3), if $K_{min} = 60 \text{ MPa}\cdot\text{m}^{1/2}$ instead of $K_{min} = 20 \text{ MPa}\cdot\text{m}^{1/2}$.

The MC computed for the TS specimens according to Eq. (1) runs higher than the experimental points for $T > -30^\circ\text{C}$ and lower for $T < -60^\circ\text{C}$. It is very different from

the exponential regression line (Fig. 7a). According to the MC concept, the fracture toughness data, when recalculated to the reference thickness $B = 25$ mm, should converge. However, this is not the case for the specimens made of the Hardox-400 steel with TS orientation (Fig. 7b). After converting the results to the reference thickness 25 mm the K_{mat} values do not converge. They increase with the specimen thickness. The data points in Fig. 7b have been received in two steps. In the first step Eq. (3) was used to plot the curve $K_{mat}(T)$ for each specimen thickness. Then the MC equation (Eq. (2)) was plotted and from these curves the data points in Fig. 7b were computed. This is opposite to the observations made for steels with yield strengths lower than 825 MPa.

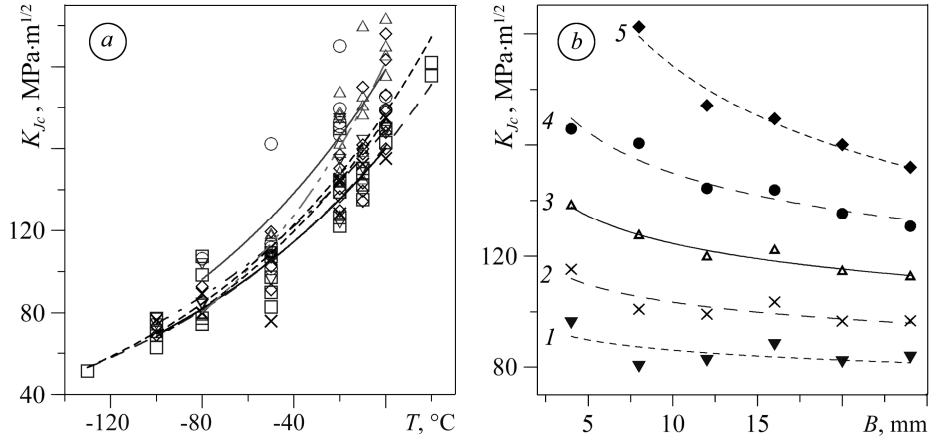


Fig. 6. Fracture toughness as a function of temperature: *a* – all data points $\{K_{Jc}; T\}$ and exponential regression lines for different specimens' thicknesses B (\circ – 4 mm; \triangle – 8 mm; \diamond – 12 mm; ∇ – 16 mm; \times – 20 mm; \square – 24 mm); *b* – K_{Jc} values vs. specimen thickness for different temperatures (set 1 – for -80°C ; set 2 – for -60°C ; set 3 – for -40°C ; set 4 – for -20°C ; set 5 – for 0°C).

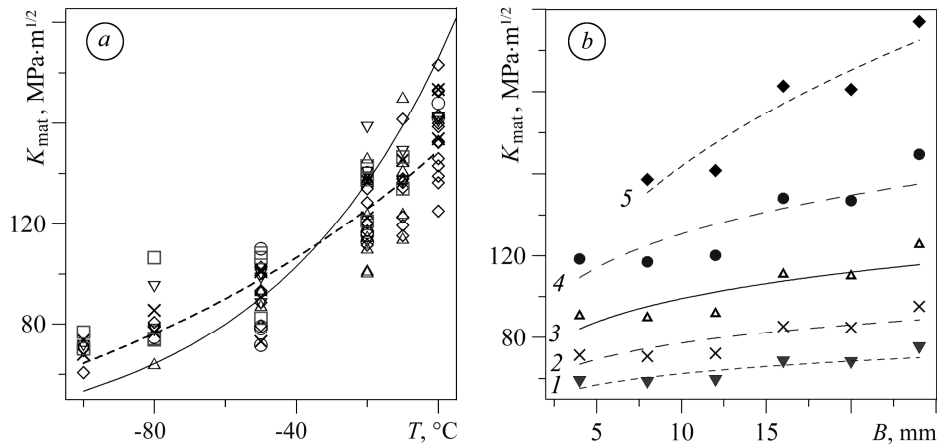


Fig. 7. Experimental data after conversion to the reference thickness 25 mm: *a* – K_{mat} vs. T , solid line is MC obtained according to Eq. (1) and dashed line is exponential regression line; *b* – K_{mat} values vs. specimen thickness, B , for various temperatures. (Symbols are the same as in Fig. 6).

Another observation following from the experimental results obtained using the specimens with TS orientation is that the curves plotted for the original thicknesses of the specimen are closer to each other than after conversion to the reference thickness of 25 mm (Eq. (1)). The values of the reference temperatures T_Q computed for different

thicknesses, B , and after conversion to the reference thickness, $B = 25$ mm, are presented in the Table. According to MC concept the reference temperatures, T_Q , after conversion to the reference thickness, $B = 25$ mm must be similar (theoretically). The data presented in the Table show a different behavior.

Reference temperature, T_Q , computed for different specimens thicknesses

Thickness, B , mm	4	8	12	16	20	24
T_Q , data for B mm	-60.22	-48.25	-45.41	-54.96	-49.89	-52.74
T_Q , data for $B = 25$ mm (Eq. (1))	-34.12	-33.33	-30.23	-47.54	-47.09	-56.29

It follows from the discussion in this section that the classical shape of the MC (Eq. (1)), derived for the ferritic steels with the yield strength $\sigma_y < 825$ MPa, is not directly applicable to the high-strength Hardox-400 steel. The results obtained for the Hardox-400 steel are similar to those for the S960QC steel [13, 14].

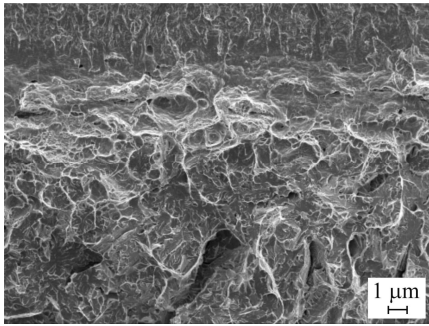


Fig. 8: Transition mechanism from ductile to cleavage fracture at $T_{\text{test}} = -10^\circ\text{C}$ for the Hardox-400 steel.

For the Hardox-400 steel, the change of the fracture mechanism from ductile to cleavage was observed for fracture toughness values equal to $K_{Jc} \approx 165 \div 170$ MPa·m^{1/2}. These values are similar to those obtained for the S960QC steel. Accordingly, the temperature of the ductile to brittle transition, T_{trans} , for the S960QC steel was established about $T_{\text{trans}} \approx -50^\circ\text{C}$ [13, 14] and for the Hardox-400 steel it was estimated as $T_{\text{trans}} \approx -10^\circ\text{C}$ (Fig. 8).

Two MC, for all data of the Hardox-400 and of the S960QC steels are shown in Fig. 9. They are computed according to Eq. 4 for $P_f = 0.5$ (curve 1), for $P_f = 0.05$ (curve 4) and $P_f = 0.95$ (curve 3). For the S960QC steel the coefficients are similar to the Hardox-400 steel, but not the same: $A + B = 35$; $C^* = 145$; $D = 0.016$ [14, 15]. For the Hardox-400 steel these coefficients are as follows: $A + B = 30$; $C^* = 145$; $D = 0.013$. For both steels the modified MC for the probability of failure $P_f = 0.5$ run very close to the regression exponential lines (curve 2).

Two MC, for all data of the Hardox-400 and of the S960QC steels are shown in Fig. 9. They are computed according to Eq. 4 for $P_f = 0.5$ (curve 1), for $P_f = 0.05$ (curve 4) and $P_f = 0.95$ (curve 3).

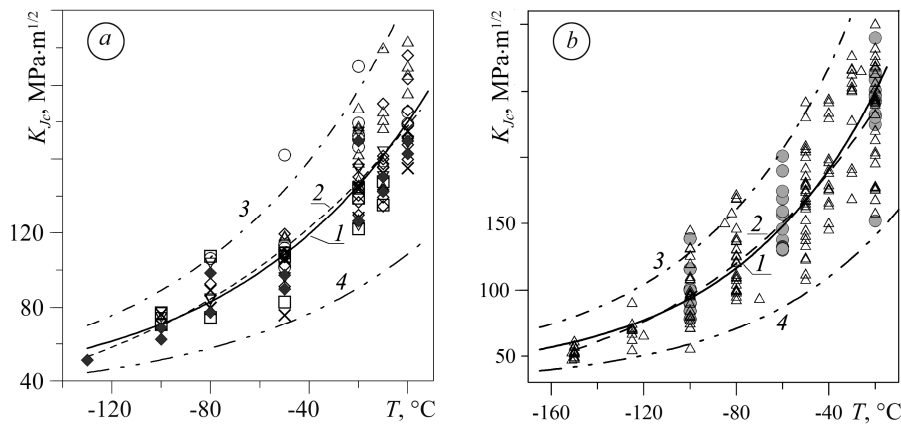


Fig. 9. Modified MC: a – for the Hardox-400 steel; b – for the S960QC steel.

CONCLUSION

It was shown that the classical MC formula (Eq. (1)), which was derived for ferritic steels with $\sigma_y < 825$ MPa, should not be used for the high-strength steels tested under this research program. The classical MC formula used for the high-strength ferritic steels S960QC and Hardox-400 does not provide a satisfactory approximation of the experimental data. As a result of the thermo-mechanical treatment and due to the microstructure variation through the plate thickness, the effect of thickness on the fracture toughness is not observed as it is in the case of the ferritic steels with yield strength less than 825 MPa.

It should be noted that the limit fracture toughness value $100 \text{ MPa}\cdot\text{m}^{1/2}$ assumed for low- and medium-strength steels is not a suitable number for the two high-strength steels S960QC and Hardox-400. If this value was used in the MC formula for the high strength steels, the transition temperature would have been about -90°C . Such information would be misleading for a customer. It was established that the transition from ductile to cleavage fracture mechanism takes place at the fracture toughness $K_{Jc} \approx 165 \div 170 \text{ MPa}\cdot\text{m}^{1/2}$ and the transition is observed at $T_{\text{trans}} = -10^\circ\text{C}$ for the Hardox-400 steel and $T_{\text{trans}} = -50^\circ\text{C}$ for the S960QC steel. It was proposed that the general shape of the MC formula should be preserved for the high-strength ferritic steels, but the coefficients entering it should be slightly changed and determined separately for each steel (Eq. (4)).

РЕЗЮМЕ. Проаналізовано тріщиностійкість високоміцних феритних сталей в інтервалі температур крихко-в'язкого переходу. Досліджено дві сталі S960QC і Hardox-400. Експериментальні результати порівняно з отриманими за стандартною формулою Master Curve (MC). Виявлено, що цю формулу можна використати для оцінювання тріщиностійкості високоміцних феритних сталей після відповідних модифікацій. Збережено структуру формули MC, але змінено коефіцієнти. Залежність між тріщиностійкістю і товщиною елемента, яку містить в стандартна формула MC, не підтверджується для високоміцних феритних сталей. Не вдалося використати одну формулу MC для різних високоміцних феритних сталей, на відміну сталей з межею міцності, нижчою від 825 МПа.

РЕЗЮМЕ. Проанализирована трещиностойкость высокопрочных ферритных сталей в интервале температур хрупко-вязкого перехода. Исследованы две стали S960QC и Hardox-400. Экспериментальные результаты сравнены с полученными по стандартной формуле Master Curve (MC). Обнаружено, что эту формулу можно использовать для оценки трещиностойкости высокопрочных ферритных сталей после соответствующих модификаций. Сохранена структура формулы MC, но изменены коэффициенты. Зависимость между трещиностойкостью и толщиной элемента, которую содержит стандартная формула MC, не подтверждена для высокопрочных ферритных сталей. Не удалось использовать одну формулу MC для разных высокопрочных ферритных сталей, в отличие сталей с границей прочности ниже 825 МПа.

Acknowledgements. Financial support from the Polish Ministry of Science and Higher Education under contract No 2014/15/B/ST8/00205 is gratefully acknowledged.

1. Wallin K. The scatter in K_{Ic} results // Eng. Fract. Mech. – 1984. – **19**, № 6. – P. 1085–1093.
2. Gao X. and Dodds R. H. Constraint effects on the ductile-to-cleavage transition temperature of ferritic steels: a Weibull stress model // Int. J. of Fract. – 2000. – **102**. – P. 43–69.
3. Joyce J. A. and Tregoning R. L. Investigation of specimen geometry effects and material inhomogeneity effects in A533B steel // Proc. ECF 14–Fracture Mechanics Beyond 2000. – Krakow. – 2002. – **Vol. II/III**. – P. 55–63.
4. Ruggeri C., Dodds R. H., and Wallin K. Constraint effects on reference temperature, T_0 , for ferritic steels in the transition region // Eng. Fract. Mech. – 1998. – **60**, № 1 – P. 19–36.
5. Дзіоба І. Р., Студент О. З., Марков А. Д. Про сучасний підхід SINTAP та його використання для оцінки робоздатності зварних з'єднань парогонів ТЕС // Фіз.-хім. механіка матеріалів. – 2005. – **41**, № 6. – С. 70–79.

- (*Dzioba I. R., Student O. Z., and Markov A. D.* On the contemporary SINTAP approach and its application to the evaluation on the serviceability of welded joints of steam pipelines of thermal power plants // *Materials Science*. – 2005. – **41**, № 6. – P. 791–804.)
6. *Дзіоба І. Р., Цирульник О. Т.* Оцінка цілісності зварних труб магістральних газопроводів за процедурами FITNET // *Фіз.-хім. механіка матеріалів*. – 2009. – **45**, № 6. – С. 57–64.
(*Dzioba I. R. and Tsyurul'nyk O. T.* Analysis of the integrity of welded pipe of gas mains by the FITNET procedures // *Materials Science*. – 2009. – **45**, № 6. – P. 817–825.)
 7. *ASTM E1921-05*. Standard test method for determination of reference temperature, T_0 , for ferritic steels in the transition range // *Annual Book of ASTM Standards*. – 2005. – **Vol. 03.01**. – 2005. – P. 1128–1147.
 8. *FITNET*. Fitness for Service Procedure / Eds.: M. Koçak, S. Webster, J. J. Janosh, R. A. Ainsworth, R. Koers. – Stuttgart: GKSS Research Centre Geesthacht GmbH, 2008.
 9. *Wallin K. and Nevasmaa P.* Structural Integrity Assessment Procedures for European Industry (SINTAP) // Sub-Task 3.2 Report: Methodology for the treatment of fracture toughness data: procedure and validation. – Report No. VAL A: SINTAP/VTT/7.VTT Manufacturing Technology, Espoo. – 1998. – 52 p.
 10. *Bannister A. C.* Structural Integrity Assessment Procedures for European Industry (SINTAP) // Sub-Task 3.3 Report: Determination of Fracture Toughness from Charpy Impact Energy: Procedure and Validation, Report No SINTAP/BS/15. British Steel plc. – 1997.
 11. *Fracture* characteristics of new ultra high-strength steel with yield strengths 900–960 MPa / P. Nevasmaa, P. Karjalainen-Roikonen, A. Laukkanen, T. Nykänen, A. Ameri, T. Björk, T. Linnell, and J. Kuoppala // *Rautaruukki Corporation*, – 2010. – 10 p.
 12. Porter D. Developments in hot-rolled high strength structural steels // *Nordic welding conference 06: New trends in welding technology*. – Finland: Tampere, 2006. – 9 p.
 13. *Neimitz A., Dzioba I., and Linnell T.* Modified master curve of ultra high-strength steel // *Int. J. of Pressure Vessels and Piping*. – 2012. – **92**. – P. 19–26.
 14. *Neimitz A., Dzioba I., and Pala T.* Master curve of high-strength ferritic steel S960QC // *Key Eng. Mat.* – 2014. – **598**. – P. 178–183.
 15. *Bainite in Steels* // Bhadeshia H.K.D.H. – London: Institute of Materials, 2001. – 458 p.
 16. *Дзіоба І. Р.* Властивості сталі 13ХМФ після експлуатації та деградації в лабораторних умовах // *Фіз.-хім. механіка матеріалів*. – 2010. – **46**, № 3. – С. 65–72.
(*Dzioba I. R.* Properties of the 13HMF steel after operation and degradation under laboratory conditions // *Materials Science* – 2010. – **46**, № 3. – P. 357–364.)
 17. *ASTM E1737-96*. Standard Test Method for *J*-Integral Characterization of Fracture Toughness. ASTM International, West Conshohochen, PA, 1996.
 18. *ASTM E1820-09*. Standard Test Method for Measurement of Fracture Toughness. – Annual book of ASTM standards, vol. 03.01; 2011. – P. 1070–1118.
 19. *Dzioba I., Pala R., and Pala T.* Temperature dependency of fracture of high-strength ferritic steel Hardox-400 // *Acta Mechanica et Automatica*. – 2013. – **7**, № 4. – P. 222–225.

Received 15.03.2016